LONDON, METEOROLOGICAL OFFICE.

Met.O.15 Internal Report No. 007.

Measurement of precipitation using the E290 weather radars. By RYDER,P. and GLOSTER,J.

London,Met.Off.,Met.O.15 Intern.Rep.No.007,[1977], 31cm.Pp.13,16 pls.

An unofficial document - not to be quoted in print.

METEOROLOGICAL OFFICE
London Road, Bracknell, Berks.

MET.O.15 INTERNAL REPORT

007

MEASUREMENT OF PRECIPITATION USING THE E290 WEATHER RADARS

by

P. RYDER & J. GLOSTER

Cloud Physics Branch (Met.O.15)

Introduction

In a further attempt to understand the performance of the E 290 radar (see Met O 15 Internal Report No. 1) the quantitative characteristics of the system are predicted on the basis of available information and the results of additional tests are reported. The expected performance is first assessed through a discussion of basic radar theory as developed by Battan (1971) and Harrold (1965).

Expected performance

1.1 Basics The standard expression linking back scattered power to radar parameters may be written as :

$$P_r = \frac{P_t L G^2 \lambda^2 \phi^2 c \tau}{512 \pi^2} \psi \frac{\Sigma\sigma}{r^2}$$

where P_M = minimum detectable power = $4.2\ 10^{-13}$ watts
(this figure is a combination of that quoted by MEL and their -7 dB 'fudge' factor)

Pr = received power

P_t = transmitted power = 30 K watts

G = antenna gain = 32 dB = $1.58\ 10^3$

λ = wavelength = 3.2 cm

ϕ = beam width = 2.8^0 = $4.9\ 10^{-2}$ radians

C = pulse length = 4 μ sec = 1.2 Km

L = radome/waveguide loss = -4dB = 0.4

ψ = fraction of illuminated volume being filled by the target

r = range of the target

$\Sigma\sigma$ = back scatter cross-section per unit volume

Thus $Pr = 2.1\ 10^{10} \psi \frac{\Sigma\sigma}{r^2}$ neglecting attenuation losses.

But $\Sigma\sigma = \frac{\pi^5}{\lambda^4} \left| \frac{\varepsilon - 1}{\varepsilon + 2} \right|^2 Z$ where $Z = \Sigma D^6$, D is the particle diameter

for the situation where it may be assumed that $\lambda \gg D$

$\left| \frac{\varepsilon - 1}{\varepsilon + 2} \right|^2 = 0.93$ for water; $= 0.18$ for ice

(note ratio is $\sim 0.2 = -7$ dB)

Precipitation intensity, p , can be related to the radar reflectivity parameter Z and hence to the back scatter cross-section (e.g. Mason (1971)) thus:

through $Z = Cp^n$ $C \simeq 220$ $n = 1.6$

p mm /hr	$Z = \sum D^6$ (mm^6/m^3)	$\sum\sigma$ cm^2/cm^3
0.5	72.6	$2.0\ 10^{-10}$
1	220	$6.0\ 10^{-10}$
2	667	$1.8\ 10^{-9}$
3	1280	$3.5\ 10^{-9}$
5	2900	$7.9\ 10^{-9}$
7	4920	$1.3\ 10^{-8}$
10	8750	$2.4\ 10^{-8}$

Then for a minimum detectable power of $4.2\ 10^{-13}$ watts and assuming that the beam is filled

$$r_{max} = \sqrt{\frac{\sum\sigma}{2\ 10^{-23}}}$$

and for p = 10 mm/hr r = 350 Km (= 189 n. miles)
p = 1 mm/hr r = 54 Km (= 29 n. miles)
p = ½ mm/hr r = 32 Km (= 17 n. miles)

Concentrating on a specific range - say 15 n. miles (= 28 Km) we can determine the signal enhancement as a function of rainfall intensity, relative to the minimum detectable power

$$\frac{Pr}{Pm} = 6.46\ 10^9\ \sum\sigma$$

p	$\Sigma\sigma$	$Pr/_{PM}$	dB
$\frac{1}{2}$	$2.0\ 10^{-10}$	1.3	1.1
1	$6.0\ 10^{-10}$	3.9	5.9
2	$1.8\ 10^{-9}$	11.6	10.6
3	$3.5\ 10^{-9}$	22.6	13.5
5	$7.9\ 10^{-9}$	51	17.1
7	$1.3\ 10^{-8}$	87	19.4
10	$2.4\ 10^{-8}$	155	21.9

This is shown in figure 1.

The doubling of rainfall intensity every 5 dB is worthy of note.

1.2 Geometry of the C.130 radar

Before considering range and attenuation effects, it is worth recalling the geometrical characteristics of the radar on the aircraft. These are demonstrated in figure 2. The beam width is $\sim 3^{\circ}$, and the radar can be directed either horizontally or to $+ 15^{\circ}$ to $- 15^{\circ}$ in 3° steps, whilst scanning a 180° arc ahead of the aircraft.

The pulse length is 1.2 Km and the beam diameter as a function of range is as follows.

Range		Beam diameter
Km	nm	Km
10	5.4	0.5
20	10.8	1.0
30	16.2	1.5
40	21.6	2.0
50	27.0	2.5
100	54.0	5.0

Beyond a few tens of kilometres the radar beam diameter becomes greater than the characteristic dimensions of several meteorological parameters - e.g. height of the boundary layer, depth of precipitating cloud diameter of updraughts in precipitating cumulus etc. Thus the assumption of an essentially uniform echo filling the pulse volume is increasingly unsound, and the meteorological value

FIG 1. Variation of Received Power with Rainfall Intensity.

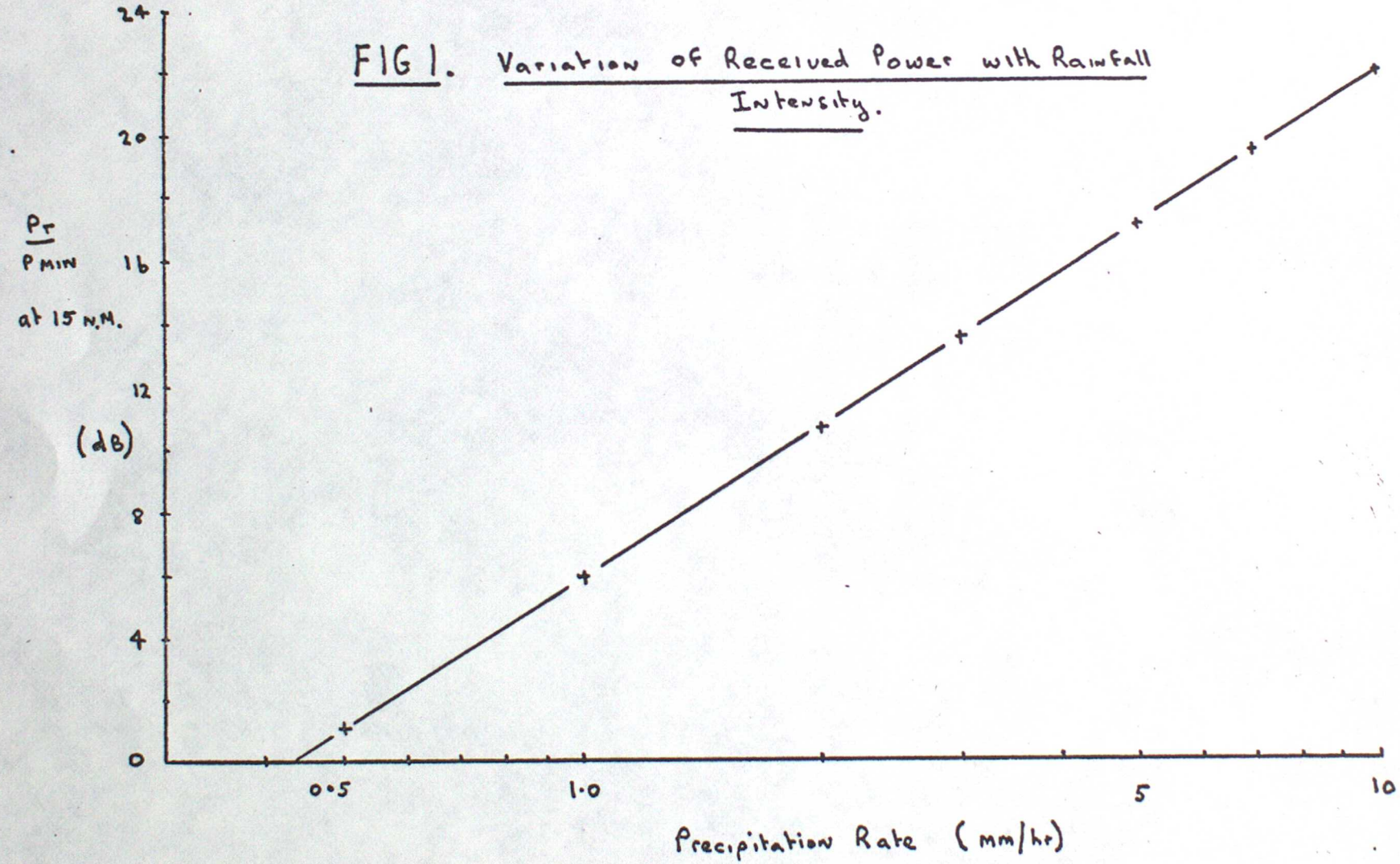

FIG 2. Radar Geometry in Flight.

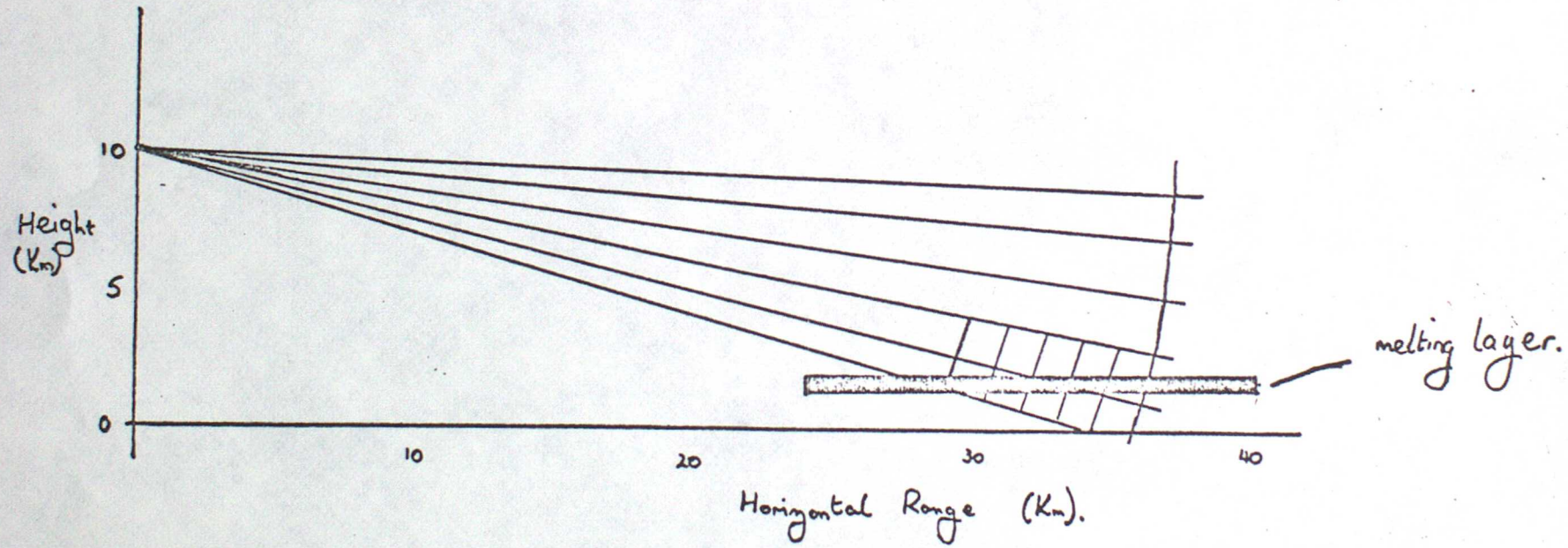

of the measurement is correspondingly reduced. It is unlikely that meaningful quantitative data can be extracted beyond $\sim$ 20 n.mile range.

It is likely that the radar will execute scans at programmed sequence of elevations/depressions or rely on forward movement of the aircraft at a fixed depression angle, to investigate the 3 dimensional characteristics of the echo. It is therefore appropriate to consider the distance between the beam and flight altitude for various tilt angles and ranges

Tilt angle	Height difference at a (Km) slant range of			
	10 Km	20 Km	30 Km	40 Km
1.5°	0.26	0.52	0.79	1.05
3.0	0.52	1.05	1.57	2.10
4.5	0.79	1.57	2.36	3.15
6.0	1.05	2.10	3.15	4.20
7.5	1.32	2.63	3.95	5.27
9.0	1.58	3.17	4.75	6.33
10.5	1.85	3.71	5.56	7.41
12.0	2.13	4.25	6.38	8.50
13.5	2.40	4.80	7.20	9.60
15.0	2.68	5.36	8.04	10.72
16.5	2.96	5.92	8.89	11.85

1.3 Range effects

Equation (1) relates the back-scattered energy to the characteristics of the scattering volume only. In reality energy will be absorbed by the material through which the radar beam passes. Thus the range dependent terms can be identified as Ψ/r^2 to account for beam divergence

where $\psi = \left(\frac{x}{\phi r}\right)^2$ for $x < \phi r$

$\psi = 1$ for $x \geq \phi r$

x is the dimension of the echo region (assumed spherical)

and $2\int_0^r \kappa \, dr$ to account for attenuation. At 3.2 cm, absorbtion by precipitation is the major source for this term and $\kappa = 7.4 \; 10^{-3} \; p^{1.31}$ - see Harrold (1965) for example.

The effect of beam divergence for features of characteristic dimensions 1 - 2 Km is shown in the table and figure 3

R(Km)	2 Km $10/R^2$	dB	=1.5 Km $10/R^2(\chi/\phi R)^2$	dB	=1.0 Km $10/R^2(\chi/\phi R)^2$	dB
10	1.00	0.0	1.00	0.0	1.00	0.0
15	0.44	-3.5	0.44	-3.5	0.44	-3.5
20	0.25	-6.0	0.25	-6.0	0.23	-6.5
25	0.16	-7.9	0.16	-7.9	0.09	-10.3
30	0.11	-9.5	0.10	-10.0	0.04	-13.5
35	0.08	-10.9	0.05	-12.6	0.02	-16.1
40	0.06	-12.0	0.03	-14.9	0.01	-18.3

The effects of precipitation attenuation are shown in figure 4. Assuming a characteristic size of frontal precipitation regions of $\sim$ 20 Km, a 3 dB error is created by $\sim$ 6 mm/hr precipitation; a not unreasonable rate for an active front. Such an error is also created by a 5 Km diameter convective cell producing 17 mm/hr.

1.4 Melting layer and ice effects

The different fall speeds of snow and rain and the dielectric coefficients of ice and water combine to create an enhanced echo intensity in the region where snow particles are melting and contracting to form rain. When effects of coagulation and drop break up are included enhancements of the order of 6 - 8 dB can be expected - see Battan (1971) for example. The effects of dielectric coefficients and fall speed are approximately equal so that in widespread precipitation, which is essentially constant with height across the melting layer, a similar echo is to be expected above and below the layer of enhancement. However, the growth of snow particles by aggregation will lead to an echo intensity which decreases with height in the ice regime. Dynamic equilibrium between coagulation and break up is expected to create an echo intensity which is more or less constant with height below the freezing level.

Fig 3. Variation of Back Scattered Energy as a Function of Range Normalised to 10 km.

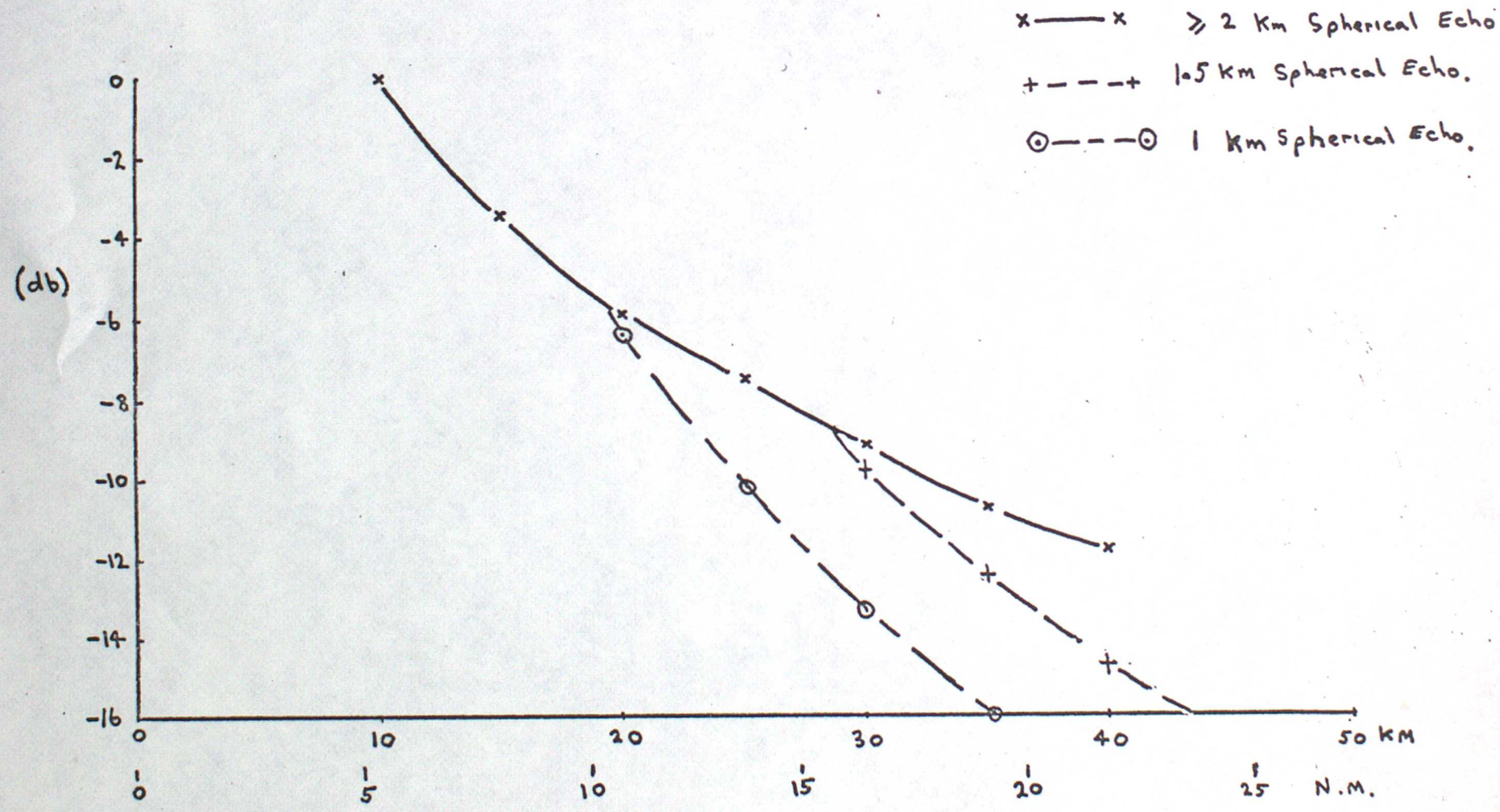

FIG 4. Variation of Two Way Attenuation with Precipitation Rate.

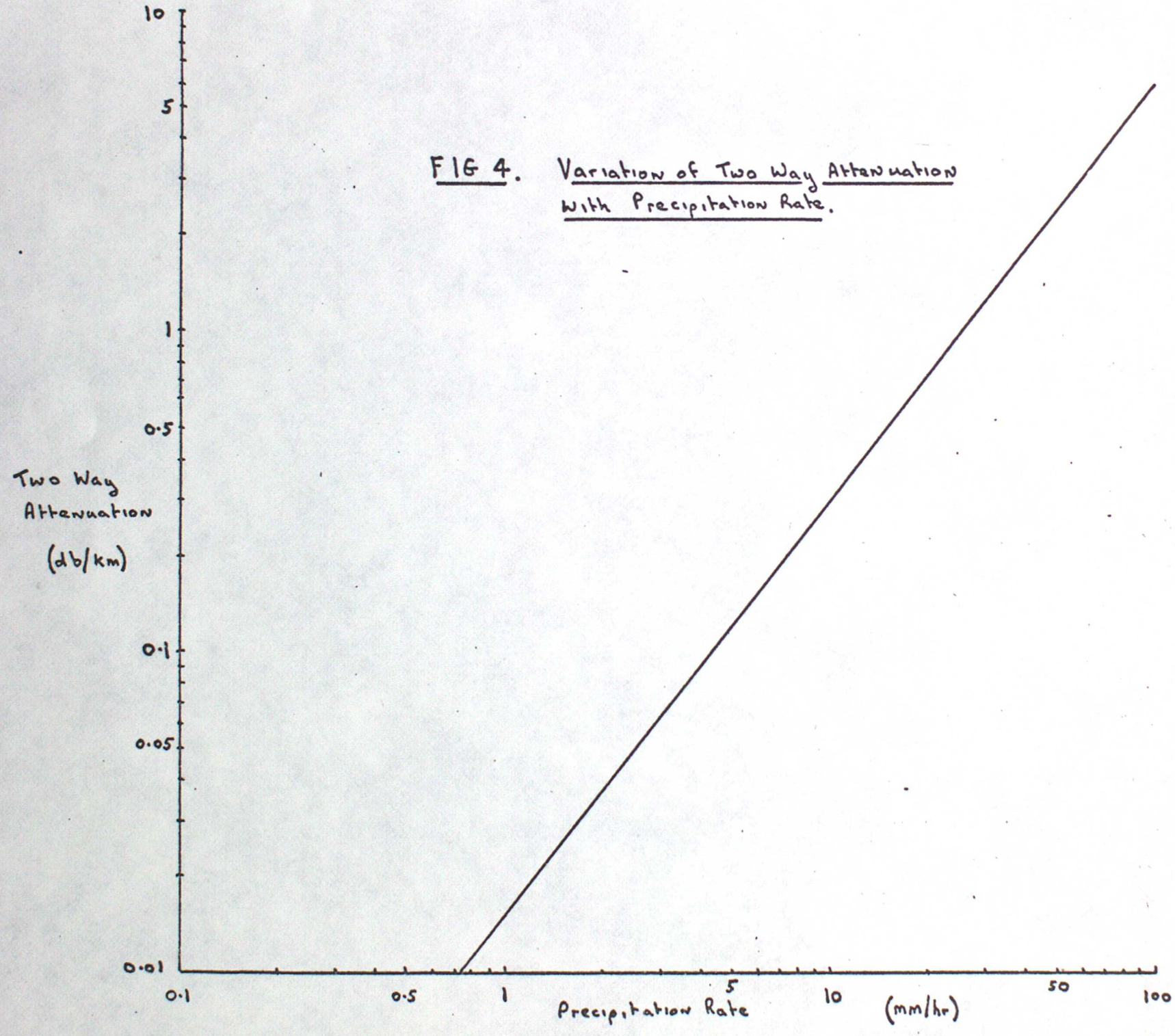

The melting layer is likely to be only 0.3 to 0.5 Km deep so that at ranges beyond ∿ 5n miles the enhanced echo will not fill the pulse volume. At 20n miles a slab echo will be reduced by 6 dB due to this effect. Thus an aircraft flying at 10 Km, looking say 15° below horizontal, may never detect the melting band. The layer will always be located at or close to extreme range and the effects of echo enhancement will be significantly reduced to say +2 to 3 dB by the non-beam filling effect. See figure 2.

1.5 Other sources of error

Stability. Harrold (1965) suggests a typical figure of ∿ 2 dB but no information exists on the performance of the C-130 radar in this respect.

Side lobe energy. Again no information is available for the E290 but provided the side lobe sensitivity is at least 15 dB below the main lobe this is not expected to be a serious source of error (∿ 1 dB).

2. Radar intercomparison

2.1 Flight trials The flight trials reported in Met O 15 Internal Report No. 1, in which the air-borne radar was made to scan areas which were also under the surveillance of a ground radar, indicated qualitative agreement between the two systems. However, data was obtained on an opportunity basis and no attempt was made at that time to maximise the common sampling volume. Accordingly a few C130 flights were undertaken in November/December 1976 in conjunction with the Met Office Radar Research Laboratory who were operating a 43S weather radar on the Gower Peninsula in South Wales. Flight plans were designed to give comparable sample volumes for both radars. Thus the C130 flew alternately towards and away from the 43S passing overhead the radar on each transit. On most runs the aircraft operated at FL 40 but on one occasion the height was FL 180. The E290 radar was operated on the 20n mile range in the WEA mode on all runs reported here. When the aircraft was at FL 40, the radar was set to scan at 0° elevation but this was changed to -6° at FL 180 so that the beam intercepted the sea surface just beyond the 20n mile range mark.

2.2 Data recording and analysis

Aircraft data were recorded as described in Met O 15 Internal Report No. 1. The analysis method was also similar except that much of the manual effort necessary before, was reduced by automating the film scanner and data logging

operations. (see annexe 1). To overcome the problem of inadequate range compensation suspected from the previous work, only data from one range was used in any single area analysis. The analysis program is described in annexe 2.

The data from the 43S were provided by MORRL in the form of areal precipitation intensities averaged over 2 x 2 Km squares horizontally and typically 1 Km vertically. A conversion from precipitation to signal intensity was made according to figure 1 with zero dB set at $\frac{1}{4}$ mm/hr; the estimated 43S threshold.

2.3 Results from flight H 172 (30.11.76)

Five aircraft runs from the twenty or so available and corresponding data from the 43S were analysed in detail. Although attempts were made to ensure that the aircraft navigation relative to the ground based radar site was as accurate as possible, errors of up to $\sim$ 1n mile must be expected.

Furthermore the accuracy to which the 43S could be set up in a geographical co-ordinate system far exceeds that available to an aircraft radar of the type used on the C130. Thus the pattern of echoes detected by both radars showed good agreement as expected, but improvements could be made by small realignment of the axes of the radar scans relative to one another. Hence, the transparent overlay of figure 5 shows the 43S echo intensity relative to that expected from a precipitation intensity of $\frac{1}{4}$ mm/hr. Figure 6(a) and (b) exhibits the equivalent E290 analysis for run 7 (the quantitative implications of level 1, 2, 3 are yet to be assessed but level 3 corresponds to a greater echo intensity than level 2 etc). Straightforward use of navigation data requires coincidence of C and D in figure 5 with C and D of figure 6, but better agreement is achieved by superimposing C and C^1 and D and D^1 ; a movement of $\sim 1\frac{3}{4}$ n miles. Differences in detail remain but this is hardly surprising. It is clear that the threshold of the E290 at 8n miles range is greater than that of the 43S and that the sensitivity of the airborne radar system is lower at 12 than at 8n miles.

Figure 7 shows the relationship between the 43S echo intensity data and E290 echo level for each analysis element in the common volume. As might be expected misalignment of the patterns, reduces the slope of the regression line. The threshold of detectability at 8n miles is between 5 and 10 dB above the 43S (i.e. $\frac{1}{2}$ to 1 mm/hr) but 10 to 12 dB above at 12 n miles. The regression slope is also somewhat greater at 12n miles although this is barely significant. Data from run 9 analysed in the same manner, figure 8, confirms the basic features noted above. The run at FL 180, analysed at 18n miles is shown in

FIG 5. Malvern Data. Run 7.

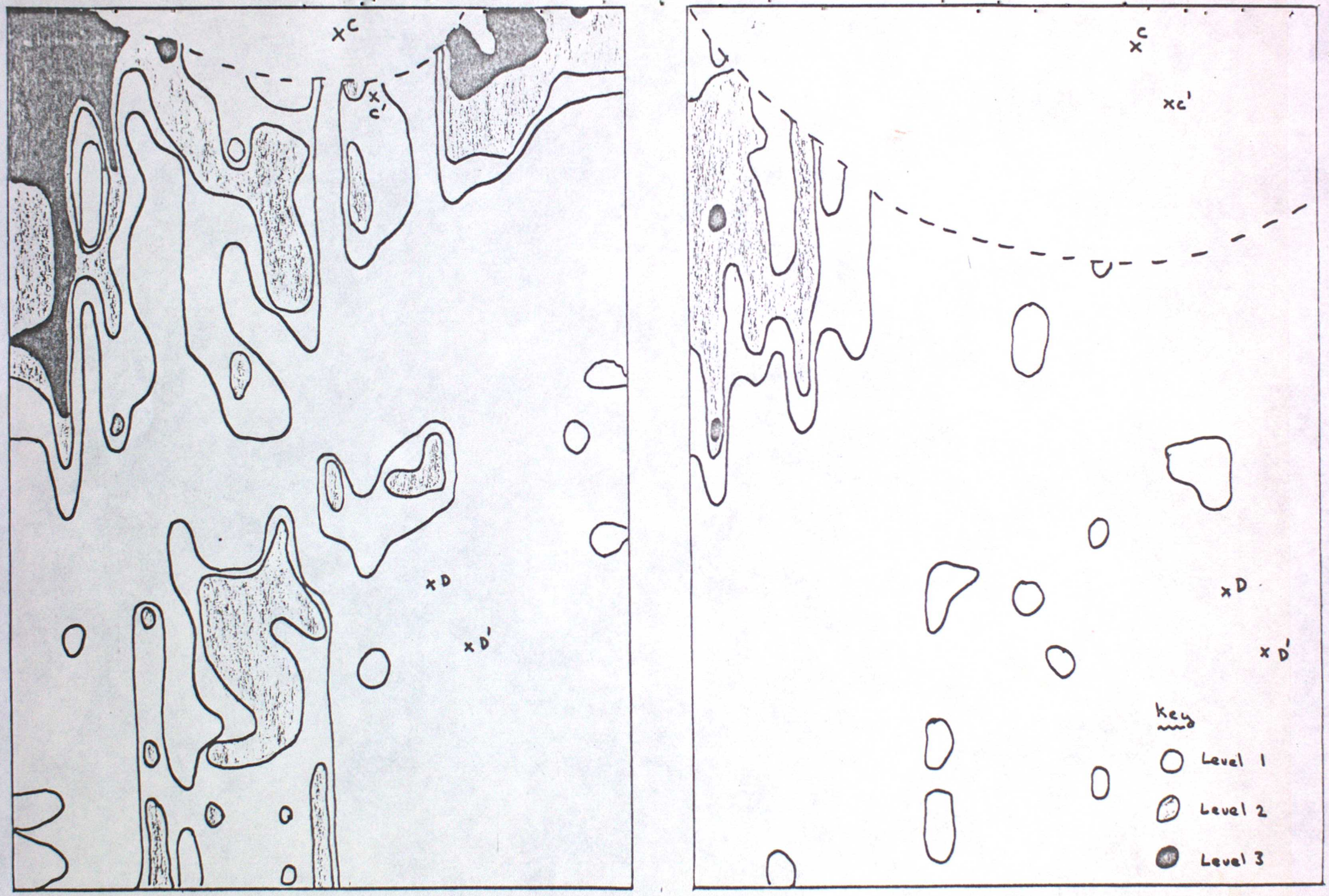

(a) 8 N.M. Analysis

(b) 12 N.M. Analysis.

FIG 6. E290 Data RUN 7.

FIG 7. Correlation of 435 and E290 Echo Intensities. Run 7.

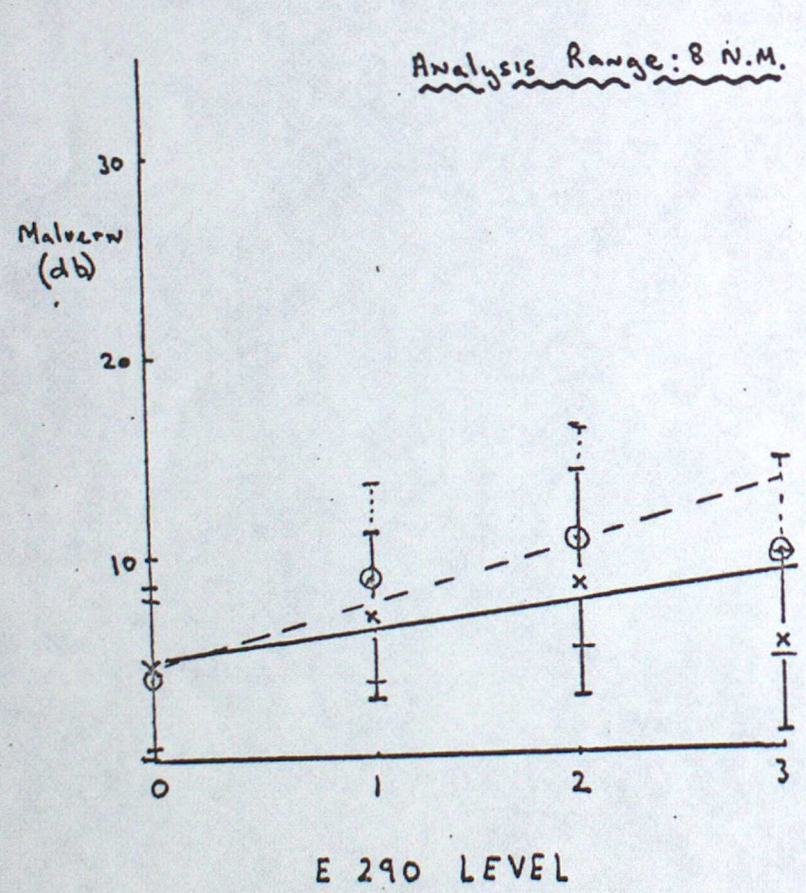

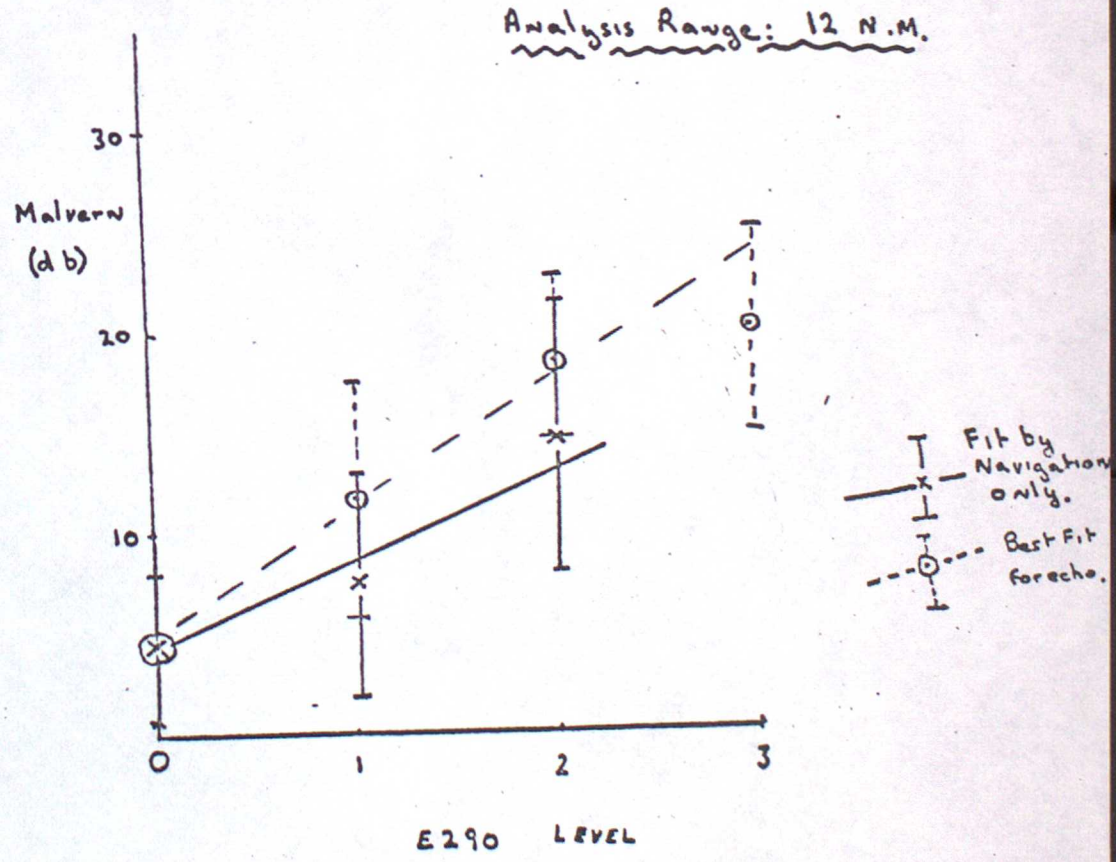

FIG. 8 Correlation of 435 and E 290 Echo Intensities. Run 9.

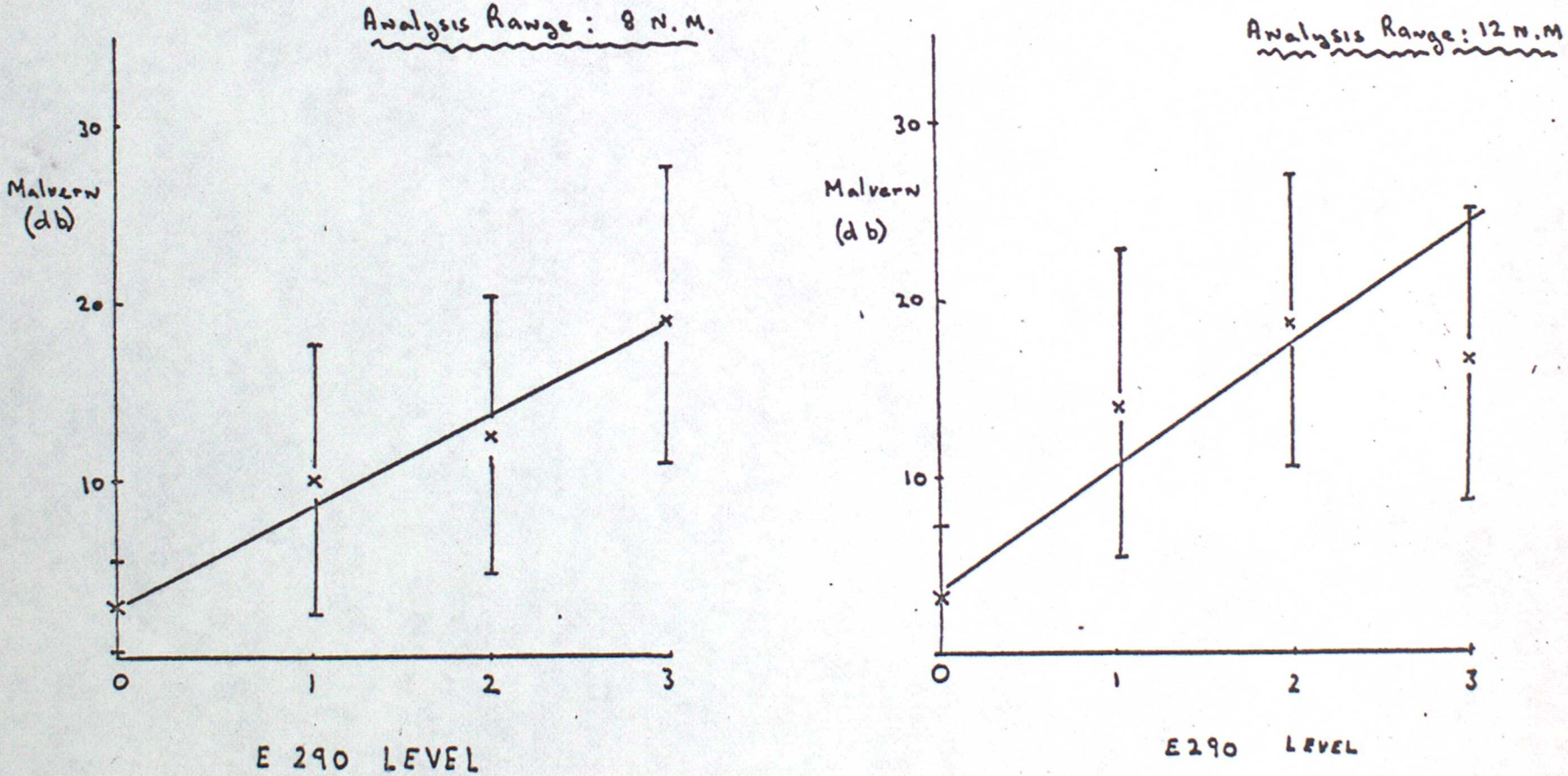

FIG. 9 Correlation of 435 and E 290 Echo Intensities.

Run 11 18 N.M Analysis Range.

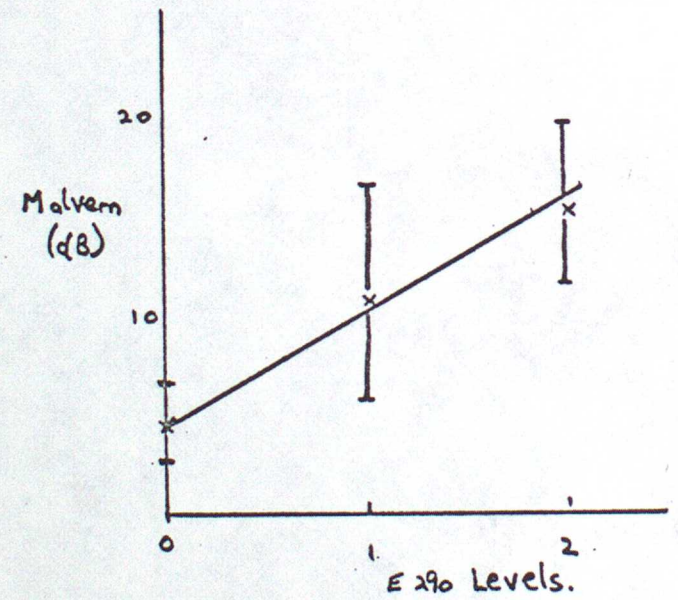

figure 9. No data at level 3 were observed on this traverse but the agreement with the earlier runs is satisfactory. This is emphasised in figure 10 where all the data on all three ranges are shown. A coherent picture emerges, in which there is a clear, if somewhat ill defined, quantitative correlation between the 43S and E290 echo level data, with differences of the order of a few dB observed between sensitivities at ranges of 8n miles and $\geqslant$ 12n miles.

The situation becomes a little less clear when a run through heavy precipitation ($\sim$ 6mm/hr) is analysed in this way. The results are shown in figure 11. There is some difficulty in identifying the source of the poor correlation between the E290 and 43S data. The effects of attenuation of the E290 beam are too small on average to account for the phenomenon although corrections of up to 6 dB are necessary in some areas of the precipitation pattern at ranges of 12n miles. The symptoms are characteristic of a mis-match between the two radar patterns as noted earlier and doubtless this could provide an explanation of the 8n mile results. The 43S precipitation intensity pattern does demonstrate considerable small scale structure in both horizontal and vertical sections. Thus the 'noise' contributed by equal intensity features which do fill and do not fill the E290 beam could also contribute significantly to the lack of correlation in this case.

3. Ground tests

As a result of the inadequacy of the range compensation suspected during H 172 and earlier flights, the range dependent gain of the system supposedly set up on 14 May 76 has been re-assessed. The results, reversed in sign and normalised to $\sim$ 20n miles are shown in figure 12. Clearly at short ranges ($\sim$ 10n miles) the correction does not have the correct form. The effect of the deficiency and finite size of an echo region can be quite significant. Thus a 1 Km diameter spherical precipitation region creates an echo enhancement of 5 dB as the aircraft moves from a range of 12 to 8n miles. The correction circuit (as measured in May 76 at least) generates a compensation of only 2 dB. Thus a relatively small echo can 'come into view' in the mid ranges as it is approached by the aircraft. The magnitude of the effect is comparable with the results of figure 10 which demonstrates a 2 to 3 dB error between the 8 and 12n mile ranges. An optimum correction can be achieved, beyond 5 n miles at least, as demonstrated by data in figure 12 which was obtained following a more recent adjustment.

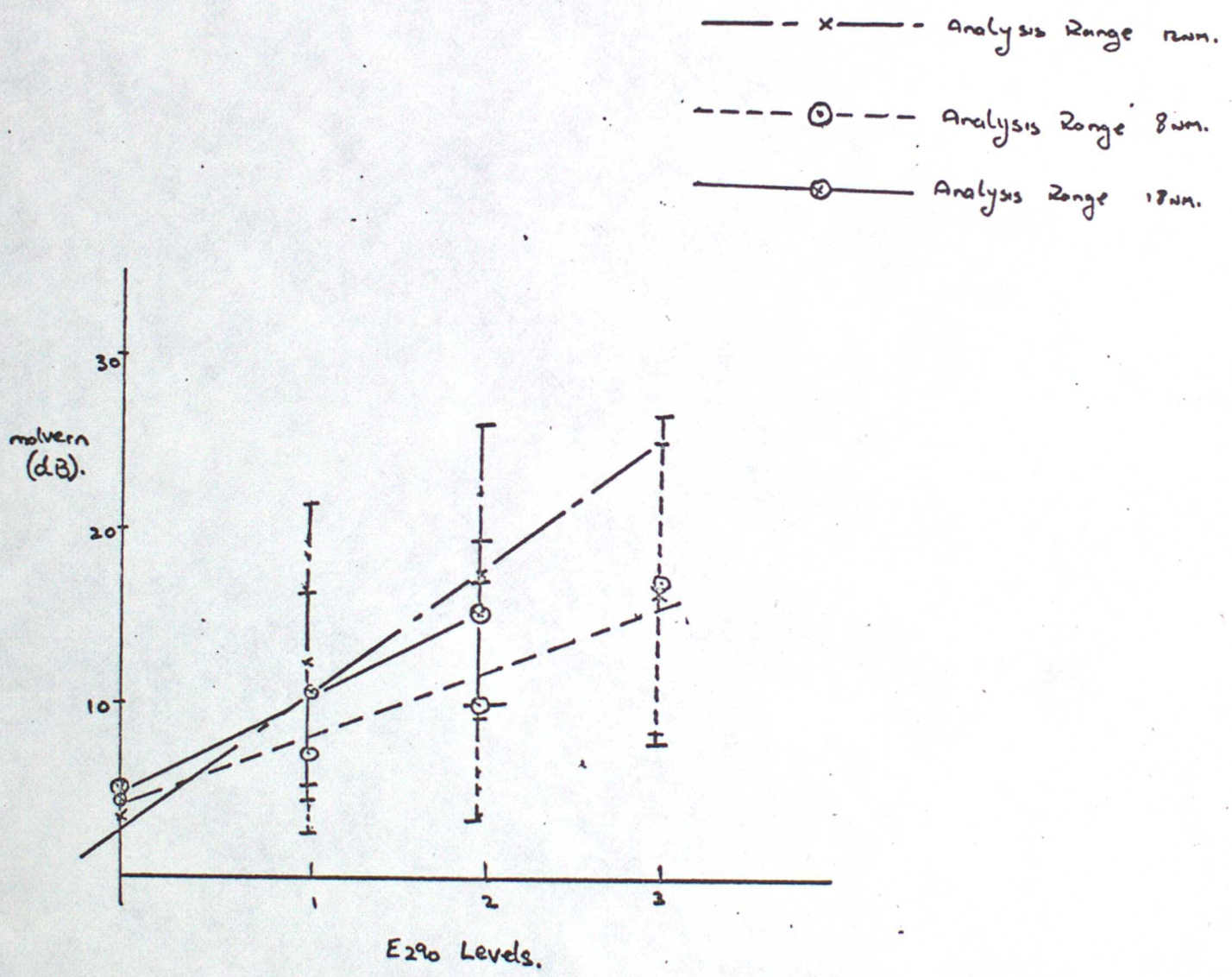

FIG. 10 Correlation of 43S and E290 Echo Intensities Runs 7, 9, 11.

FIG. 11 Correlation of 435 and E290 Echo Intensities. Run 12.

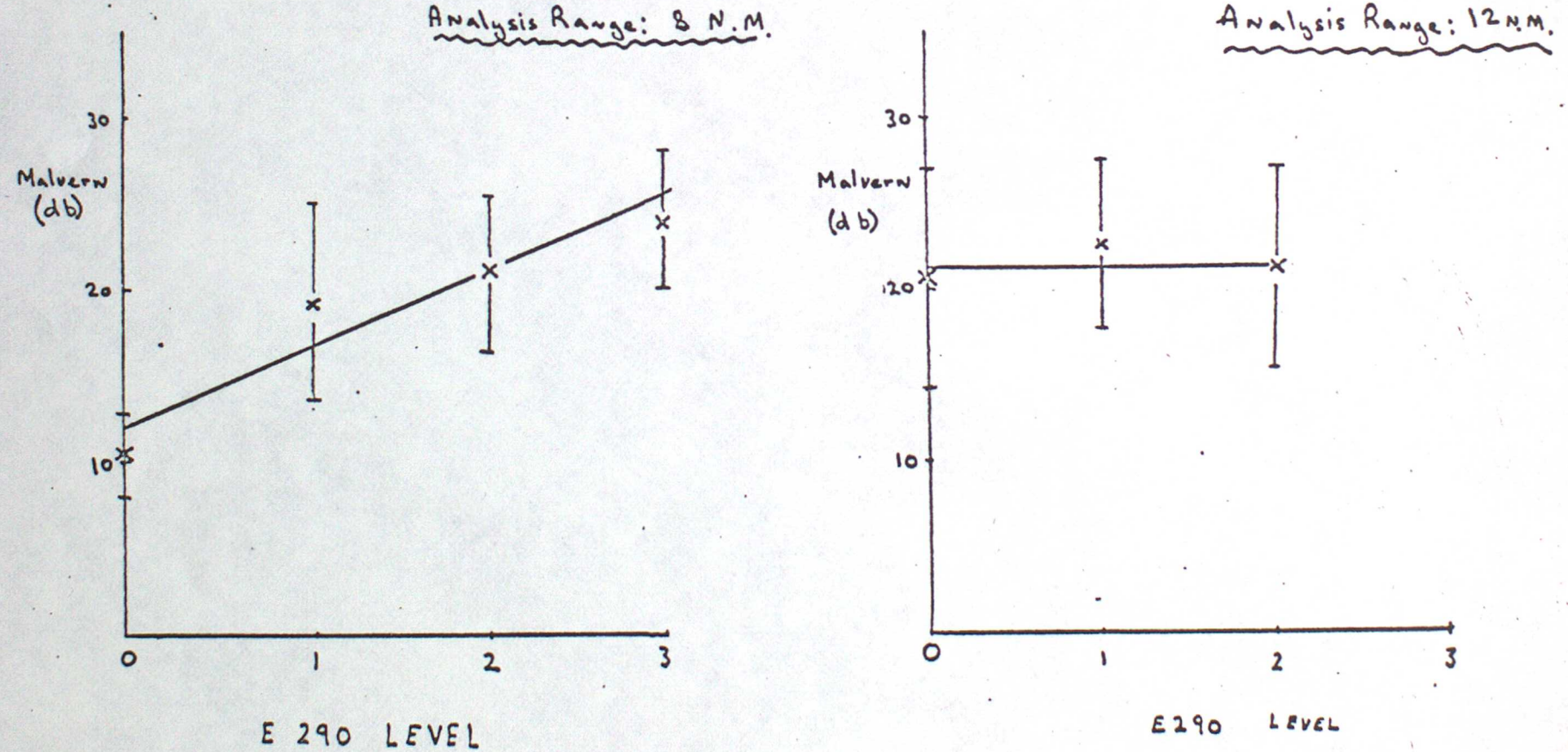

4. Conclusions

With some reservations about use in widespread heavy rainfall the E290 radar clearly can be used to map precipitation patterns. A threshold of rainfall intensity of between $\frac{1}{2}$ and 1 mm/hr has been achieved but optimisation of the range compensation circuit may reduce or increase this. Clearly the radar has some potential for quantitative precipitation intensity estimation; at least over a restricted dynamic range. The stability of any calibration is unknown and some care, above that normally applied to the radar, will doubtless be necessary to realise this potential. As discussed in section 1 and as confirmed by the results of section 2 and 3 there are several sources of error of $\sim$ 2 - 3 dB. Accordingly it is probably not justifiable to attempt quantitative resolution below $\sim$ 5 dB.

Almost certainly a complex on-line digitisation system is not justified for this radar but the semi subjective optical techniques used in this and the earlier report leave much to be desired for anything approaching routine use. The major problem arises from the great difficulty of maintaining a meaningful calibration through the display - film - photogrammetry process. Probably the simplest method of overcoming this, is to use an on-line stepped attenuator to create the quantitative capability whilst using an optical analysis technique which simply distinguishes between 'light' and 'dark'. Some form of automation in the scanning and data capture process would appear desireable.

5. Recommendations

1) Methods of monitoring the long term stability of the radar in important areas such as the transmitted power level, overall system gain, range compensation etc should be investigated.

2) The possibility of incorporating an attenuator capable of $\sim$ 5 dB steps in the radar in such a way as to maximise the available dynamic range, should be studied. It is envisaged that in flight a program of attenuation and radar elevation angle changes would be created much as elevation angles are scanned at present.

3) Photogrammetry methods should be reviewed.

FIG. 12 Variation of Back Scattered Energy as a Function of Range, Showing the Normalised Gain of the Echo Equalisation Circuit (Reversed in Polarity to Illustrate Conformity).

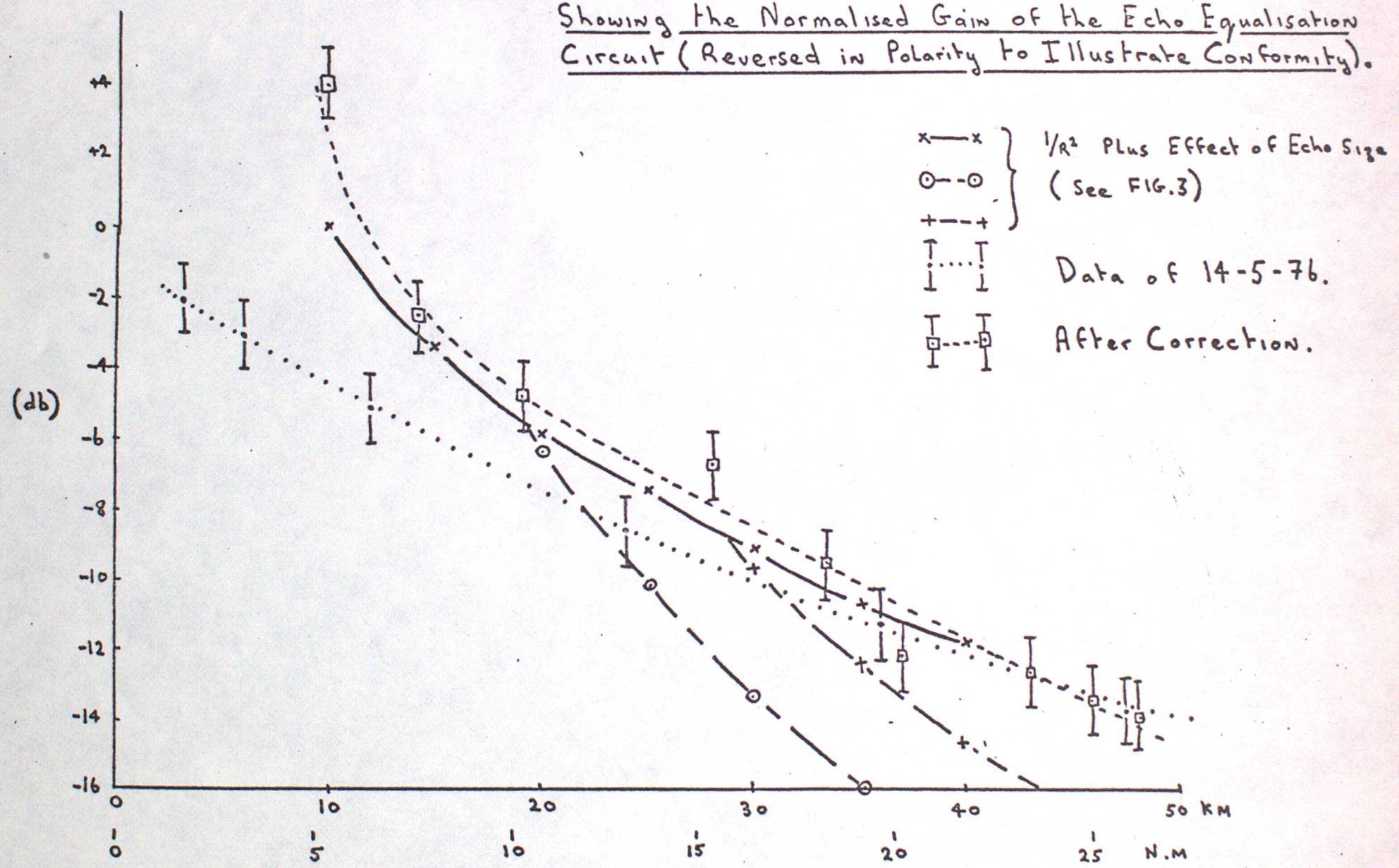

ANNEXE 1 Electronic System (see Fig. A1) by G Cromarty

1. Intensity of Echo Measuring System

The picture to be analysed is projected onto a disc mounted on the spindle of a stepper motor. A phototransistor located in a radial slot on the disc can be preset to the required radar range value. Output from the transistor circuit is fed via a buffer amplifier to the inputs of three comparators. The threshold levels of the comparators are independently adjustable. Thus the intensity of light falling on the phototransistor is converted into a voltage. The voltage is assigned one of four levels depending on the threshold of the comparators. A combinational logic circuit encodes the comparator outputs into a 2 bit binary signal for recording purposes.

2. Motor Drive System

The motor assembly consists of a 0.75° per step motor driving a 1 : 10 gear box giving 7.5° per step on the disc. Motor phase control is provided by a single SAA 1027 I.C. which also gives a reversing facility. Drive pulses are sent in groups of "N" so that the disc rotates 7.5 N° at a time. After a short pause to allow the disc to reach equilibrium a strobe is issued to MPX I to latch the 2 bit reading and then the next group of pulses is issued. This process repeats until the disc has rotated through 7.5 M N° at which point a reverse stream is generated and the motor drives the disc back until a stop on the disc reaches an indexing microswitch. Both "M" and "N" are presetable on thumbwheel switches. When the disc has returned to the index position no further action takes place until a manual start is initiated.

3. Data Multiplexing and Recording System

When the start button has been pressed information is multiplexed to the cassette recorder by a 4 channel multiplexer MPX II. Initially the preset information is recorded as channels 1, 2 and 3 of MPX II. The multiplexer then halts on channel 4 and the motor drive system is enabled. As 2 bit intensity readings are taken the information is multiplexed into the latches by selectively strobing the latches using MPX I. Each time 8 bits of information have been accumulated in the latches a 9 bit byte is recorded on the cassette, parity being added prior to recording. The latching and recording sequence then continues until the scan is complete. As a result the data is recorded in the following format :

Byte 1	BCD ANGLE	BCD UNITS OF HOURS
Byte 2	BCD 10s of MINUTES	BCD MINUTES
Byte 3	BCD 10s of SECONDS	BCD SECONDS
Byte 4	1st 2 BIT ECHO,	2nd 2 BIT ECHO, 3rd 2 BIT ECHO, 4th 2 BIT ECHO
Byte 5	5th 2 BIT ECHO,	6th 2 BIT ECHO, 7th 2 BIT ECHO, 8th 2 BIT ECHO
	ETC.	

In operation Byte 1 is preceeded by a manually introduced inter block marker for data manipulation purposes.

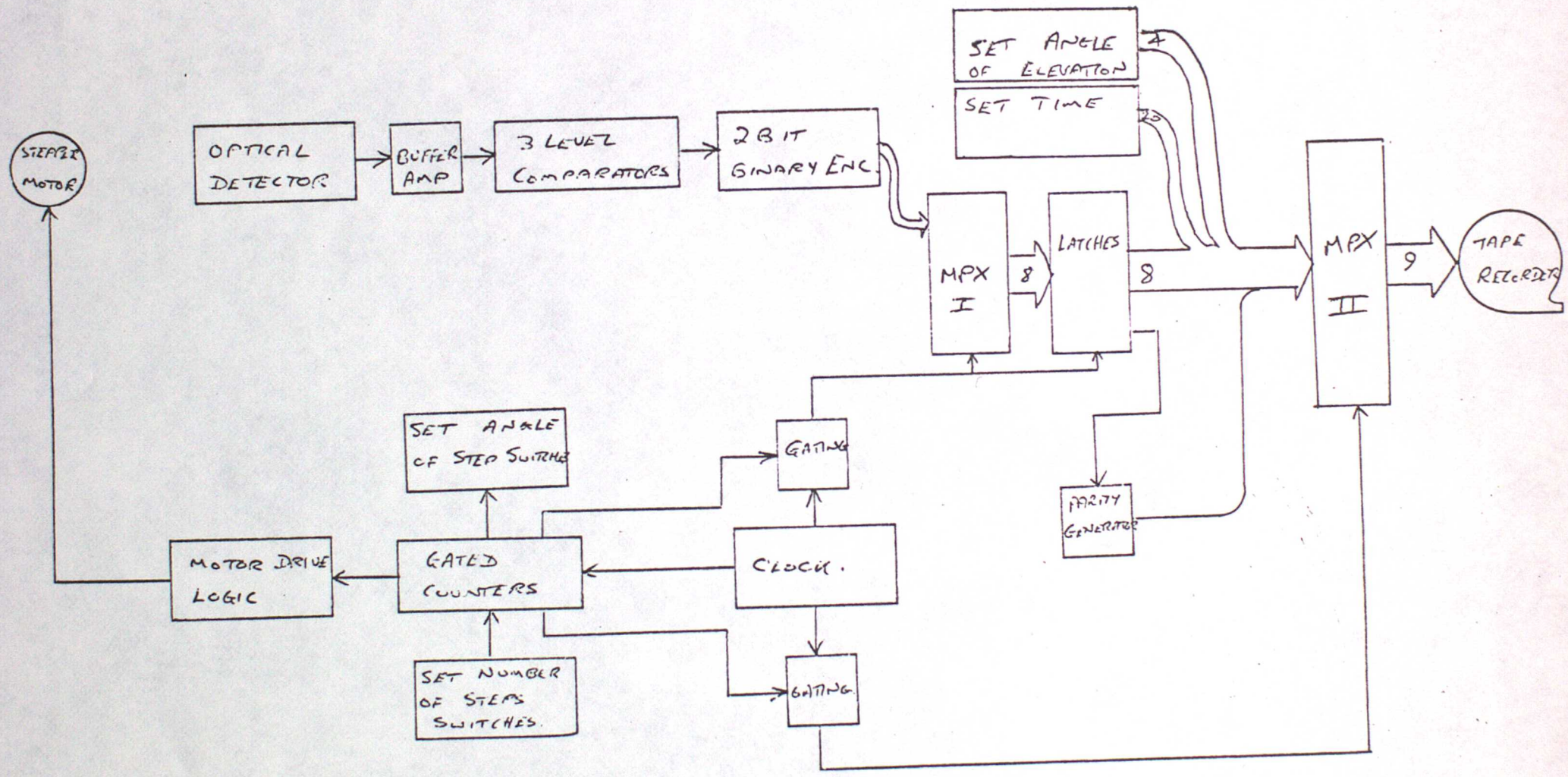
SET ANGLE OF ELEVATION
4
SET TIME
23
STEPPER MOTOR
OPTICAL DETECTOR
BUFFER AMP
3 LEVEL COMPARATORS
2 BIT BINARY ENC
MPX I
8
LATCHES
8
MPX II
9
TAPE RECORDER
SET ANGLE OF STEP SWITCHES
GATING
PARITY GENERATOR
MOTOR DRIVE LOGIC
GATED COUNTERS
CLOCK
SET NUMBER OF STEPS SWITCHES
GATING

FIGURE A.1

ANNEXE 2

Description of the computer program used to analyse the E290 data

by :- R. Allt

1. KRAB is a programme which performs a metmerge on to KRAG, which is at present a member of M15. SOURCELIB on SYS 003 (ON line). Purpose of the KRAB is to read the data from an IBM tape, covert it from bits to decimals, and store it in two offline (MET 009) data sets, M15. KIDJA and M15. KRALA having eliminated records with parity errors.

Input IBM tape (RADAR 1) and data cards (these give title, number of words, number of data points per frame and run number).

Output

(a) Datasets.

M15. KIDJA : Sequential dataset on disk (1 cylinder, VBS format, block size 2000).

M15. KRALA : Sequential dataset on disk (1024 bytes, VBS format, block size 1024).

The array ID is read to KIDJA once for each radar picture analysed.

ID (1) is the angle of elevation of the radar beam in degrees.
ID (2) gives the time of the picture.
ID (3), (4) spare.
ID (5) and above contain the data, i.e. the intensity of radar echo at each point that was measured on the picture.

The array LA is read to KRALA at the end of the data.

LA (1) = N PMAX.
LA (2) - LA (11) contains the frequencies of the angles of elevation of the radar beam (i.e. from - 12° to + 15° respectively).
LA (12) is spare.
LA (13) is the date.
LA (14) is the run number.
LA (15) gives the total number of records written to KIDJA (in effect the sum of the frequencies of the angles of elevation).

(b) Written

Parameter bit index.
Listing of last I/P data block.
Raw data.
List of data from tape.
List of array L A and each array I D which has been transferred to KIDJA and KRALA.

2. KRAD. is a programme which performs a metmerge on to KRAD PLO, which is at present a member of M15. SOURCELIB on SYS 003 (on line).

Purpose of KRAD is to retrieve information from the offline datasets M15. KRALA and M15. KIDJA, and produce a diagrammatic representation (on paper) of the intensities of radar echo at any one height by the aircraft, as shown by the radar.
N.B. For a given KRALA and KIDJA, a diagram will be produced for each angle of elevation of the radar beam, but range of analysis is constant throughout.

Input

M15. KRALA and M15 KIDJA are supposed to exist.
Data cards giving for each run the co-ordinates and names of the start and end positions, also the time, both true and coded, for these positions, the aircraft height in feet, and the range of analysis.

Analysis of Radar Data — Relation Between KRAB and KRAD

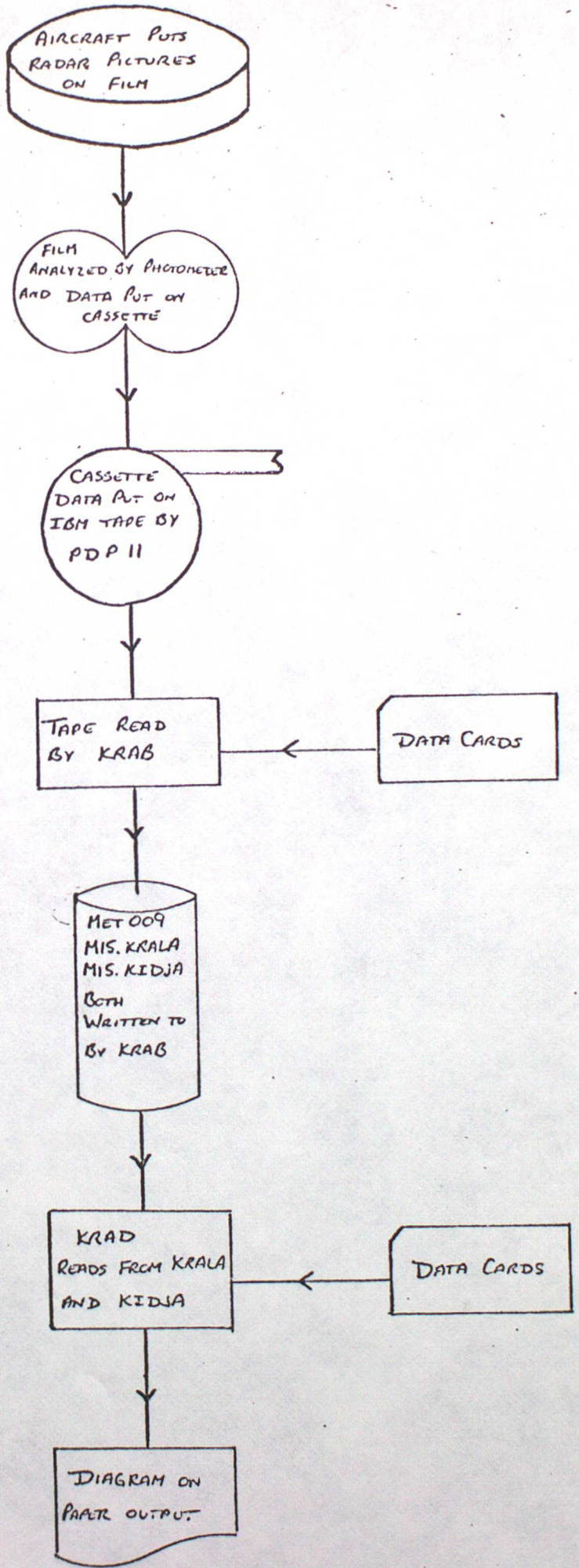

FLOW-CHART FOR KRAD

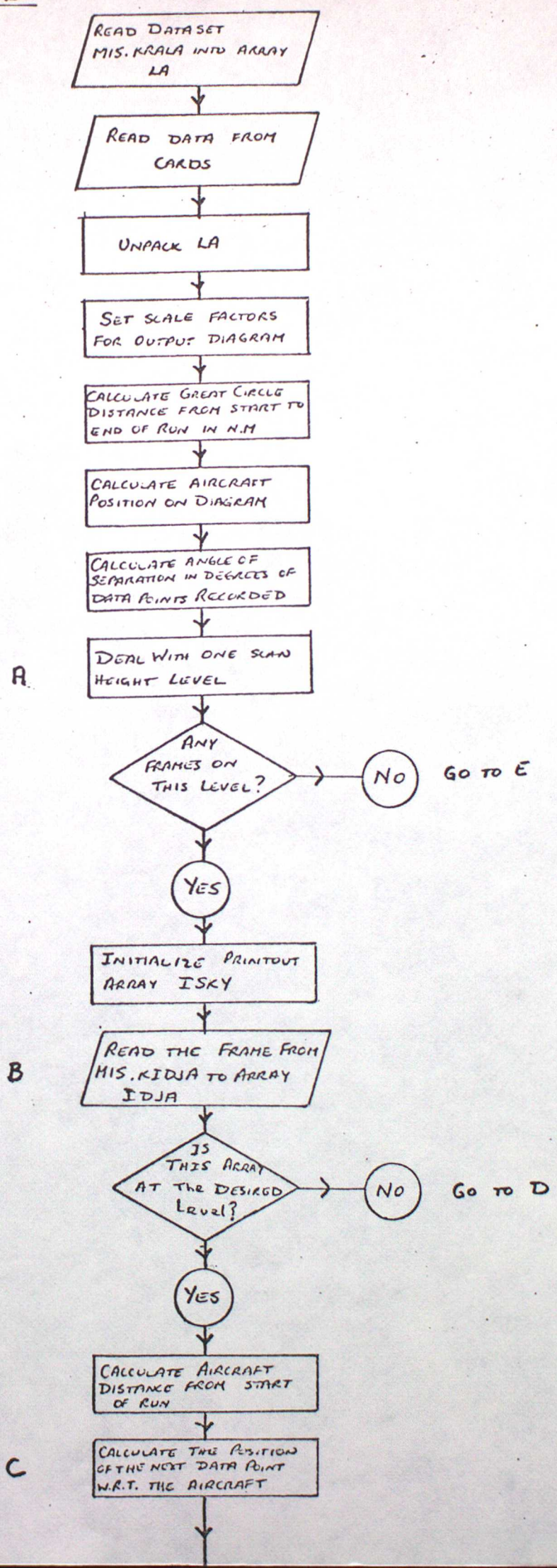

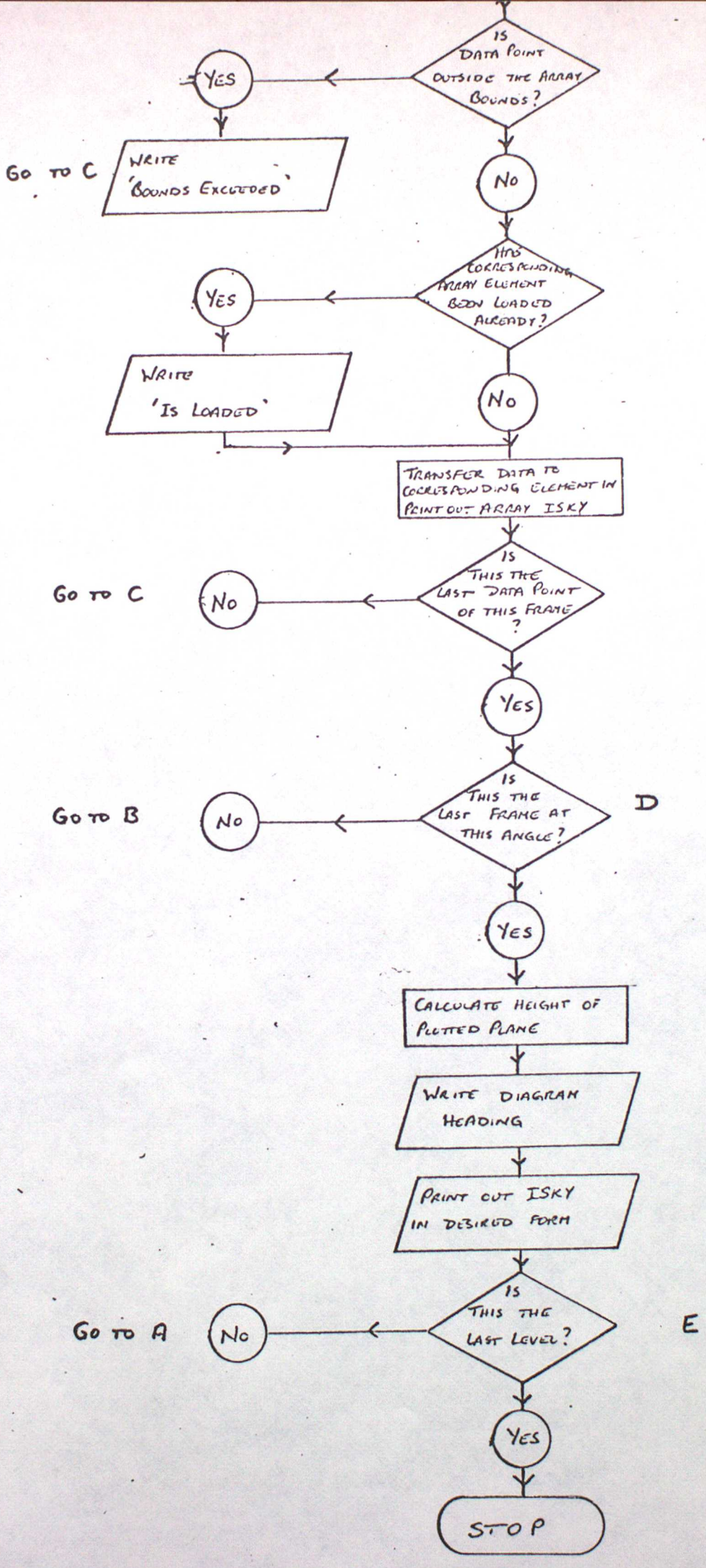
IS DATA POINT OUTSIDE THE ARRAY BOUNDS?
YES
NO
GO TO C
WRITE 'BOUNDS EXCEEDED'
HAS CORRESPONDING ARRAY ELEMENT BEEN LOADED ALREADY?
YES
NO
WRITE 'IS LOADED'
TRANSFER DATA TO CORRESPONDING ELEMENT IN PRINT OUT ARRAY ISKY
IS THIS THE LAST DATA POINT OF THIS FRAME ?
GO TO C
NO
YES
IS THIS THE LAST FRAME AT THIS ANGLE?
GO TO B
NO
D
YES
CALCULATE HEIGHT OF PLOTTED PLANE
WRITE DIAGRAM HEADING
PRINT OUT ISKY IN DESIRED FORM
IS THIS THE LAST LEVEL?
GO TO A
NO
E
YES
STOP